04

Absorption of laser radiation energy in the laser-plasma radiation source with gas-jet targets

© V.E. Guseva, I.G. Zabrodin, A.N. Nechai, A.A. Perekalov, N.I. Chkhalo

Institute of Physics of Microstructures, Russian Academy of Sciences, 607680 Nizhny Novgorod, Russia e-mail: valeriegus@ipmras.ru

Received June 16, 2024 Revised February 25, 2025 Accepted February 27, 2025

The present study is taken to measure absorption of radiation of Nd: YAG-lasers with impulse duration $3.8-12.5\,\text{ns}$, the impulse energy $0.2-0.8\,\text{J}$ in laser-induced breakdown of gas jets which are formed when the gas outflows through a supersonic conical nozzle with the critical section of $500\,\mu\text{m}$, the length of 5 mm and the flare angle of 9° . It also investigates integral and time dependences of absorption of laser radiation by plasma formed on the targets of molecular (CO₂, CHF₃, CF₄, N₂) and inert (Ar, Kr, Xe) gases on their pressure at the nozzle inlet and the laser impulse energy. For the various gas targets a portion of absorbed laser energy was from $25\,\%$ to $85\,\%$.

Keywords: gas-jet target, laser impulse, nozzle, gas outflow, absorption of radiation.

DOI: 10.61011/TP.2025.07.61447.192-24

Introduction

In connection with recent achievements in developing soft X-ray mirrors with high reflectances at the wavelengths around 11 nm [1–3],it is possible to manufacture a nanolithograph using a laser-plasma source (LPS) of extreme ultraviolet (EUV) radiation with the xenon-based gas-jet target. Despite the fact that the wavelength of 10.8 nm corresponds to a peak position of the radiation band formed by the Xe ions IX–XIII, it was shown in the paper [2] that performance of the lithograph operating at the wavelength of 11.2 nm can be quite high due to use of Mo/Be multilayer X-ray mirrors.

The recent 25 years have seen a large number of investigations dedicated to various aspects of formation of EUV radiation on the various gas-jet targets [4-10]. Many studies pay greater attention to measuring intensity of EUV radiation and conversion efficiency of LPS [2,11] as well as to various aspects of LPS optimization [12]. At the same time, successful development and optimization of the powerful laser-plasma EUV radiation source requires experimentally determined parameters of processes in a laser spark such as absorption of laser radiation at the various experimental conditions. Also important are both integral absorption characteristics allowing constructing a plasma energy balance as well as time absorption dependences taken to determine the time of generation of the laser spark. Substantially less attention is paid to this issue in the literature [13-16]. It is worth noting the paper [14] among the studies dedicated to measurement of a portion of laser energy absorbed by the gas-jet targets. The said paper has investigated absorption of laser energy in plasma created

on ultrasound gas-jet targets and demonstrated effective absorption in plasma of inert gases [17].

The present study is dedicated to investigating absorption of laser radiation by the gas-jet target formed during ultrasound outflow of the gas into vacuum. These investigations were performed by means of two experimental methods. The first method was to measure integral energy of laser radiation upstream and downstream the gas-jet target by means of calorimeters. Thus, the portion of plasmaabsorbed energy of laser radiation was measured depending on the pressure of the gas-target at the nozzle inlet and on energy of the laser impulse. The second method was taken to investigate oscillograms of the laser impulse before and after interaction with the gas-jet targets by means of p-i-n-diodes and the oscilloscope having high time resolution. The gas-jet targets were formed by using the molecular (N2, CO2, CHF3) and inert (Ar, Kr and Xe) gases.

Experimental method

During the experiments, plasma was formed in the gasjet targets by using two impulse Nd: YAG- lasers with the operating wavelength of 1.064 μm and the impulse energy to 0.8 J with the various impulse duration. A diameter of the focal spot was $\sim 60\,\mu m$, while the power density in the focus spot was approximately $10^{12}\,W/cm^2$. The work was performed in an installation described in the paper [18] and specially modified for performing these experiments. The diagram of the research installation is shown in Fig. 1.

Radiation of the laser I was directed to the first dividing plate 2, whence the small portion of radiation was declined to hit the calorimeter IMO-2 3 designed to measure the

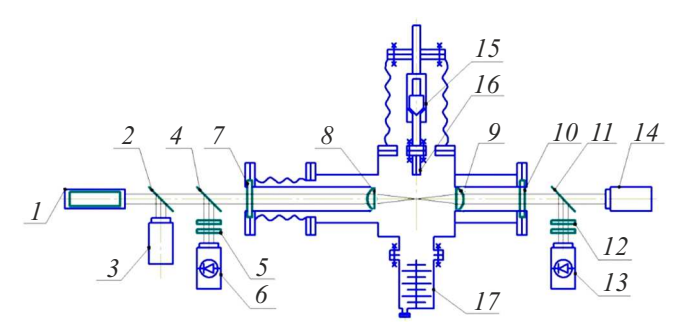


Figure 1. Schematic diagram of the installation: I — the laser; 2, 4, 11 — the dividing plates; 3, 14 — the calorimeters OIMO-2; 5, 12 — the filters; 6, 13 — the p-i-n- diodes; 7 — the inlet window; 8 — the focusing lens; 9 — the converging lens; 10 — the outlet window; 15 — the impulse valve; 16 — the nozzle; 17 — the turbomolecular pump.

energy of incident laser radiation. After the first dividing plate, laser radiation was directed to the second dividing plate 4, whence the small portion of radiation was declined and directed through the filters 5 to the p-i-n-diode (LSIP D-A40) 6 designed to record the laser impulse oscillogram Further on, laser radiation was directed into a volume of the vacuum chamber through the inlet window 7 and then focused by the lens 8 (the focal distance of 45 mm) to the gas-jet target formed by means of the ultrasound conical nozzle 16, at the distance of 0.5 mm to a nozzle exit. The nozzle opening time was adjusted by the impulse valve 15. The vacuum chamber was depressurized by means of the turbomolecular pump 17. Th focused laser radiation caused breakdown in the gas jet. The laser radiation transmitted through the gas breakdown area was converged by the lens 9 and directed through the outlet window 10 to the third dividing plate 11. The small portion of radiation that is reflected from the plate was directed through the filters 12 to the p-i-n-diode 13 designed to record the oscillogram of the laser impulse transmitted through the breakdown area. The large portion of laser radiation transmitted through the dividing plate 11 was directed to the second calorimeter IMO-2 14 designed to record energy of transmitted laser radiation.

The studied gases were fed into the chamber through the conical ultrasound nozzle with the impulse valve based on the injector Bosch 0280158017. The diameter of the critical nozzle section was $d_{\rm cr}=500\,\mu{\rm m}$, the nozzle length $L=5\,{\rm mm}$, the flare angle $\alpha=9^{\circ}$. For the inert gases, concentrations of particles in an area of generation of the laser spark were: for the pressure of $10\,{\rm bar}$ — about $1.3\cdot 10^{19}\,{\rm particles/cm^3}$, and for the pressure of $20\,{\rm bar}$ — about $2.7\cdot 10^{19}\,{\rm particles/cm^3}$ [19]. The chamber was depressurized by the turbomolecular pump of performance of $1000\,{\rm l/s}$.

The laser radiation energy was determined by means of the calorimeters IMO-2. The relative error of measurement of integral absorption was $\sim 4\%$. The laser

impulse oscillograms were recorded by means of the p-i-n-photodiodes (LSIP D-A40). The signal from the p-i-n-photodiodes was directed to amplifiers with the transmission band 1 MHz-3 GHz and then recorded by the oscilloscope RIGOL MSO8204 with the transmission band of 2 GHz. In front of the photodiodes, there were optical filters designed to reduce a radiation flux in order to avoid overloading of the photodiodes and distortion of a shape of the recorded impulses. Due to a various optical path to the p-i-n- diodes and a various length of connection cables to the oscilloscope, there was observed substantial difference in time for time of arrival of the signals from the various p-i-n-photodiodes to the oscilloscope inlet. When constructing Fig. 2, a-e, the oscillograms of these impulses were shifted in accordance with a design delay time, and for accurate alignment of the advanced impulse fronts there were manual corrections. In manual correction, the impulse shift was below 1 ns. This diagram made it possible to perform measurements with the time solution not worse than 0.5 ns.

In order to adjust the nozzle position in relation of the area of laser radiation focusing, the Bragg mirror spectrometer described in detail in [20] was additionally connected to the installation. The spectra of the studied gases were previously measured by the authors in their papers [21–23]. It was adjusted so as to obtain a maximum signal for the band (11.2 ± 0.2) nm in the EUV range. This adjustment corresponds to a position of the laser spark along the nozzle axis for all the inert gases except for xenon, for which the maximum of intensity of the EUV signal corresponds to a shift of the spark in relation of the nozzle axis [24].

In all, two sets of the experiments were carried out. The first set included measurement of a portion of the absorbed energy of laser radiation when generating the spark on the various gas-jet targets depending on the gas pressure at the nozzle inlet and the energy of incident laser radiation. The laser with the impulse duration of 7.8 ns and the impulse energy of $0.8\,\mathrm{J}$ was used. The portion of the plasma-absorbed laser energy α was determined as

$$\alpha = \frac{E_0 - E_{tr}}{E_0} = 1 - \frac{E_{tr}}{E_0},$$

where E_0 — the energy of incident laser radiation, E_{tr} — the energy of transmitted laser radiation. Hereinafter, the incident laser impulse is an impulse of laser radiation before interaction with the target. The transmitted laser impulse is an impulse of laser radiation, which is recorded after interaction with the target and leaving the vacuum chamber.

All the three processes are observed during interaction of laser radiation with plasma — absorption, reflection and refraction of laser radiation. Taking into account that laser plasma formation itself is associated, first of all, with the process of absorption of laser radiation, then the processes of reflection and refraction of laser radiation are secondary in relation to the process of absorption of laser radiation. Previously, reflection and refraction of laser beams when

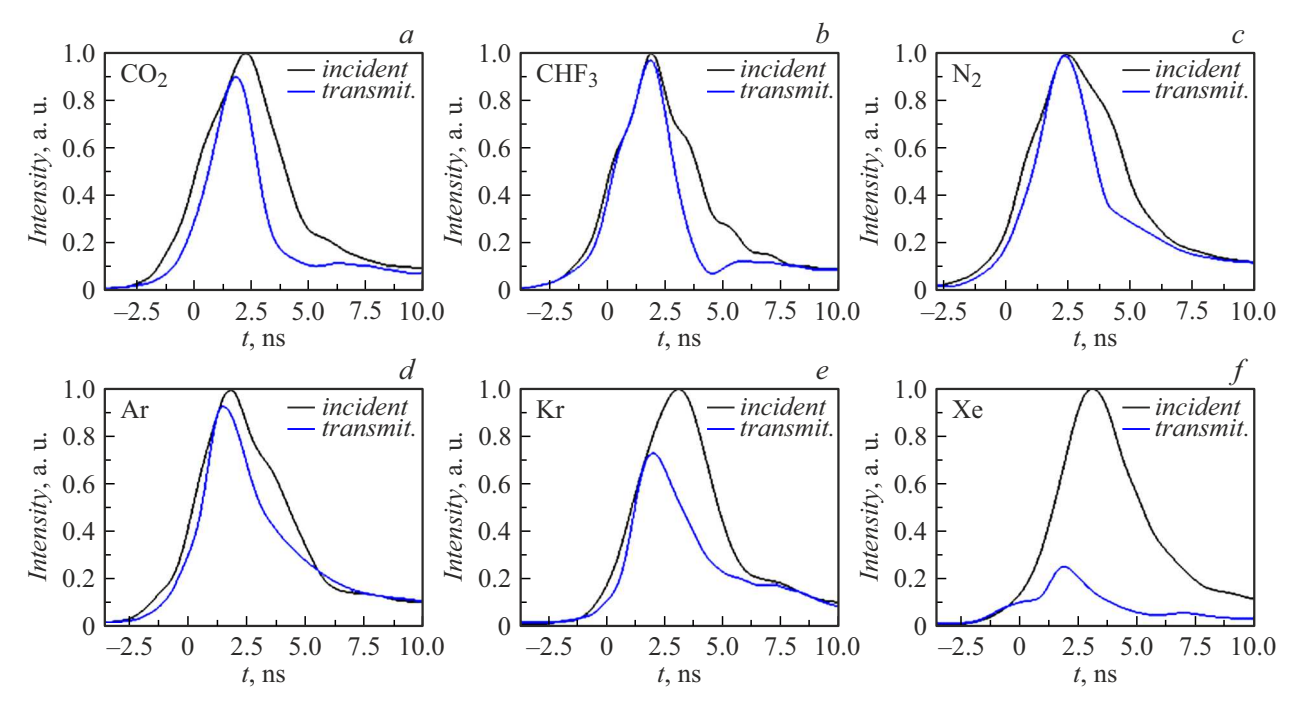


Figure 2. Oscillograms of the incident laser impulse and laser impulse transmitted through the breakdown area for the targets of $CO_2(a)$, $CHF_3(b)$, $N_2(c)$, Ar(d), Kr(e), Xe(f).

the laser spark is formed with using the similar laser system had been already investigated, for example, in the study [25]. Herein, the reflected radiation has been evaluated as $\sim 7\,\%$ of incident radiation and refraction is determined to be small. Thus, the study [25] has shown that 90 % of laser radiation which interacted with the laser spark was absorbed in it. It is assumed herein that laser radiation is either absorbed by plasma or transmitted through it, while the processes of reflection and scattering are insignificant. The error related thereto significantly reduces importance of the conducted investigation, but, however, the presented results are of interest for considering the processes in the laser sparks.

The second set of the experiments included comparisons of the oscillograms of incident laser impulses and laser impulses transmitted through the breakdown area on the gases pressure at the nozzle inlet. During the second set of the experiments, the laser with nominal impulse duration of 4.2 ns and the impulse energy of 0.8 J was used.

2. Results and discussion

Fig. 3 shows results of the measurements of the portion of laser radiation energy, which is absorbed by laser plasma. The investigations were performed for the gas-jet targets of Ar, Kr, CO₂, N₂, CHF₃ and CF₄. In these experiments, the energy of an exciting laser impulse was 0.8 J, and the impulse duration was 7.8 ns.

It is clear that for the molecular and inert gases there are different dependences of the portion of absorbed energy

on the gas pressure. Argon and krypton have an observed smooth growth of the portion of absorbed energy up to the pressure of 25 bar, while the portion of absorbed laser energy at the pressure of 25 bar is 67% for the krypton target and 50% for the argon target. For the molecular gases with increase of the gases pressure at the nozzle inlet, the absorption growth is sharper and has a trend of going to absorption with the nozzle inlet gas pressure 20-25 bar, wherein the portion of absorbed laser energy is $\sim 43\%$ for the targets of carbon dioxide and freons. The differences are observed for the nitrogen target, for which the portion

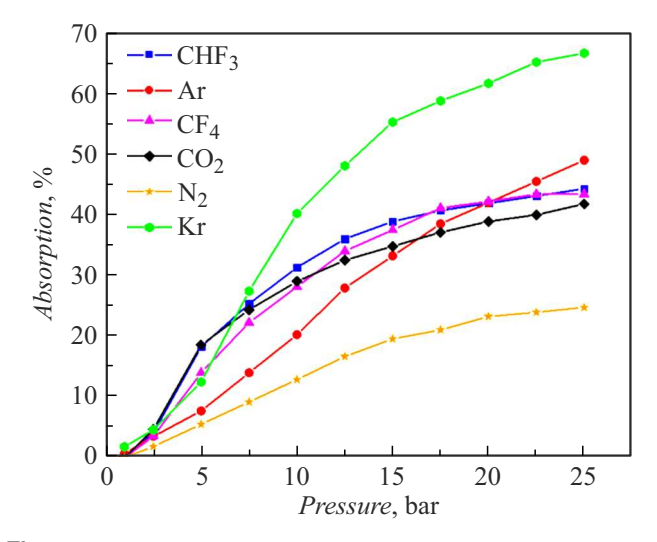


Figure 3. Portion of the laser radiation energy, which is absorbed in the laser spark, depending on the gas pressure.

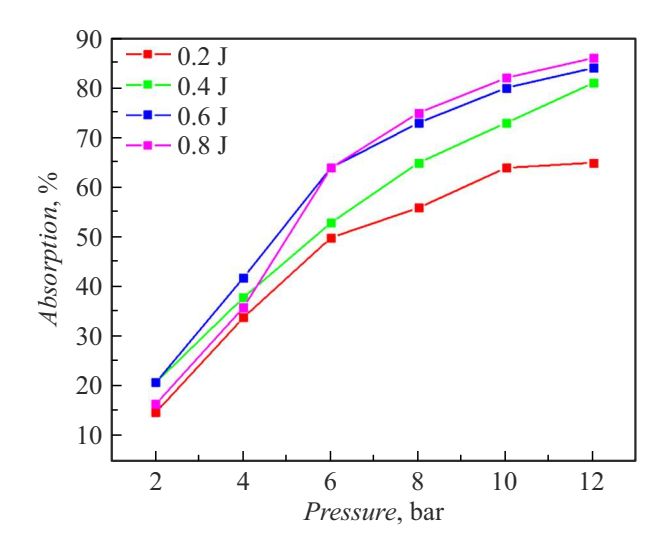


Figure 4. Portion of the laser radiation energy, which is absorbed in xenon plasma, depending on the gas pressure and the laser impulse energy.

of absorbed energy is significantly less (at the pressure of 25 bar it is 25%) than for carbon dioxide and freons at the similar type of the dependence.

The results of measurement of the portion of laser radiation absorbed energy by xenon-based plasma are shown on Fig. 4. The experiments were performed at the different gas pressures at the nozzle inlet $(2-12\,\mathrm{bar})$ and with the laser impulse energies $0.2-0.8\,\mathrm{J}$. The maximum value of the gas pressure at the nozzle inlet, at which the investigations were performed, is due to a residual pressure level in the vacuum chamber of the installation. For our depressurization system, with the nozzle inlet xenon pressure of 12 bar the chamber residual pressure was $\sim 1\,\mathrm{Pa}$, thereby resulting in strong absorption of EUV radiation by residual xenon and significant reduction of the recorded EUV signal. Thus, it makes no sense to further increase the gas pressure at the nozzle inlet with the used system of depressurization of the vacuum chamber.

With the selected method of adjustment of the laser impulse energy, the impulse full width at half maximum increases with reduction of its energy. Thus, with the laser impulse energy of $0.8\,\mathrm{J}$, the impulse full width at half maximum was $7.8\,\mathrm{ns}$, with $0.6\,\mathrm{J}-8.9\,\mathrm{ns}$, with $0.4\,\mathrm{J}-10.0\,\mathrm{ns}$, and with $0.2\,\mathrm{J}-12.5\,\mathrm{ns}$.

It is obvious that for xenon (Fig. 4) the type of dependence of the absorbed energy portion on the gas pressure at any laser impulse energies is similar to the type of dependence for the other investigated inert gases (Fig. 3). The portion of the laser radiation absorbed energy by the xenon target reaches quite high values ($\sim 80\%$ at the pressure of 10-12 bar) and it relatively weakly depends on the laser impulse energy.

Fig. 2 shows oscillograms of the incident laser impulse and the laser impulse transmitted through the breakdown area for the investigated gas-jet targets. In this set of

Measured full widths of the incident laser impulses and the laser impulses transmitted through the various targets at half maximum

Gas	CO ₂	CHF ₃	N_2	Ar	Kr	Xe
$ au_{incid}^{FWHM} \ au_{trans}^{FWHM}$	3.9 2.4	3.8 2.7	4.1 2.7	4 2.9	3.8 2.9	3.8 2.5
$\tau_{trans}^{FWHM} / \tau_{incid}^{FWHM}$	0.61	0.71	0.66	0.72	0.76	0.66

the experiments, the Nd: YAG-laser with nominal impulse duration of 4.2 ns was used, whereas the impulse energy was 0.8 J. The gases pressure at the nozzle inlet was 8 bar. The shown impulse oscillograms are provided as a result of averaging of several impulses.

The measurements were performed for the gas-jet targets of CO_2 (Fig. 2, a), CHF_3 (Fig. 2, b), N_2 (Fig. 2, c), Ar (Fig. 2, d), Kr (Fig. 2, e) and Xe (Fig. 2, f). The intensities are rated in such a way that areas under the curves are proportional to energies of the incident laser impulses and transmitted laser impulses which are measured in the previous set of the experiments. It is clear from the oscillograms of Fig. 2 that in its form the transmitted impulse is similar to the incident one, whereas there is observed narrowing of the transmitted impulse in comparison with the incident one.

The full width of the incident and transmitted laser impulses at half maximum somewhat varied during the experiment. The obtained values of the FWHM-impulses are shown in the table.

As it is obvious from the table, the full width of the incident laser impulse at half maximum (FWHM) varied from 3.8 to 4.1 ns. With formation of plasma in the targets of the various gases, FWHM of the transmitted laser impulse is from 2.4 to 2.9 ns. At the same time, a ratio of the transmitted impulse full width at half maximum to the incident impulse full width at half maximum varies within 61%–76%. For the various gas-jet targets, FWHM-of the impulse transmitted through the laser spark is approximately constant, thereby indicating a similar breakdown mechanism in the various gas-jet targets. Spread of the observed full widths at half maximum is related, in the first place, to a quite high error of the measurements.

The time passed from a start of interaction of the gas-jet target with laser radiation to generation of the absorbing plasma can be evaluated by the transmitted laser impulse full width at half maximum. Originally, the gas-jet target is almost transparent and laser radiation is transmitted through the gas target without substantial absorption [25]. Then, plasma generated by the substance of the gas-jet target becomes actually nontransparent for laser radiation and almost the entire laser energy is absorbed by plasma. The absorbed energy of laser radiation is spent for heating of the generated laser plasma, propagation of the shock waves in the gas-jet target and radiation of laser plasma [25,26].

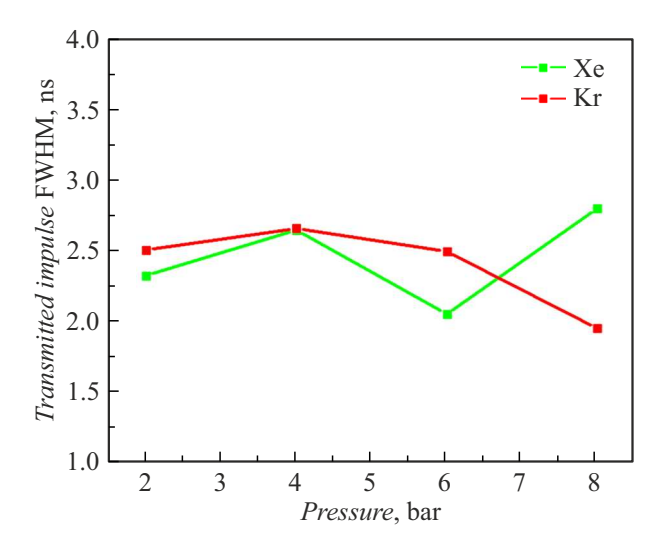


Figure 5. Dependences of FWHM of the laser impulse transmitted through the breakdown area for the targets based on xenon and krypton on the gas pressure at the nozzle inlet.

FWHM of the laser impulse transmitted through the laser spark area was separately investigated for the targets based on xenon and krypton at the various gases pressures at the nozzle inlet. The obtained dependencies are shown in Fig. 5.

It is clear from Fig. 5 that the time of generation of breakdown in xenon and krypton (which corresponds to the full width of the laser impulse transmitted through the spark area at half maximum) almost does not depend on the gas pressure at the nozzle inlet. Taking into account the errors of the performed measurements, it can be concluded that the time of generation of absorbing plasma for krypton and xenon at the various gases pressures at the nozzle inlet is almost constant and is $\sim 2.5 \, \mathrm{ns}$.

Conclusion

The present study provides the experimental dependences of the portion of absorbed energy of laser radiation by the various gas-jet targets of the molecular CO_2 , CHF_3 , CF_4 , N_2 and inert gases Ar, Kr, Xe when they outflow from the supersonic conical nozzle with the critical section of $d_{\rm cr} = 500\,\mu{\rm m}$, the length of $L = 5\,{\rm mm}$ and the flare angle of $\alpha = 9^{\circ}$. The gases pressure at the nozzle inlet was from 2 bar to 25 bar. The excitation was done by the Nd:YAG lasers with the various energy and impulse duration.

It has been established that the portion of laser radiation absorbed energy for the inert gases is 50%-60%, for carbon dioxide and freons — about 40%, for nitrogen — about 25% with the gases pressure of 25 bar at the nozzle inlet and the power density of laser radiation in the focal spot about $10^{12}\,\mathrm{W/cm^2}$. For xenon, absorption of laser radiation is 80% at the pressure of about $12\,\mathrm{bar}$ at the nozzle inlet.

When investigating the oscillograms of the incident laser impulses and the laser impulses transmitted through the

laser spark area, we have managed to evaluate the time of generation of absorbing plasma in the gas-jet targets of krypton and xenon, which was $\sim 2.5\,\mathrm{ns}$ at the gases pressures of $\sim 8\,\mathrm{bar}$ at the nozzle inlet and with excitation by the laser impulses of duration of several nanoseconds with the power density of laser radiation in the focal spot about $10^{12}\,\mathrm{W/cm^2}$.

It can be concluded from the performed study that for further investigation of intensity of EUV radiation and increase of the ratio of conversion of laser radiation into EUV radiation in the LPS sources, it is necessary to perform studies in the following fields:

- 1) investigation of the breakdown mechanisms in the jet targets to reduce the time of generation of absorbing plasma;
- 2) optimization of the shape of the laser impulse of exciting radiation;
 - 3) optimization of the parameters of the gas-jet target.

Funding

This study was supported by a grant from the Russian Science Foundation N° 22-62-00068. The system for recording the time characteristics of the laser impulses was made under state assignment FFUF-2024-0022.

Conflict of interest

The authors declare that they have no conflict of interest.

References

- R.M. Smertin, N.I. Chkhalo, M.N. Drozdov, S.A. Garakhin, S.Yu. Zuev, V.N. Polkovnikov, N.N. Salashchenko, P.A. Yunin. Opt. Express, 30 (26), 46749 (2022). DOI: 10.1364/OE.475079
- [2] N.I. Chkhalo, S.A. Garakhin, A.Y. Lopatin, A.N. Nechay, A.E. Pestov, V.N. Polkovnikov, N.N. Salashchenko, N.N. Tsybin, S.Y. Zuev. AIP Advances, 8 (10), 105003 (2018). DOI: 10.1063/1.5048288
- [3] E.A. Vishnyakov, D.L. Voronov, E.M. Gullikson, V.V. Kondratenko, I.A. Kopylets, M.S. Luginin, A.S. Pirozhkov, E.N. Ragozin, A.N. Shatokhin. Kvant. elektron., 43 (7), 666 (2013) (in Russian).
- [4] H. Fiedorowicz, A. Bartnik, M. Szczurek, H. Daido, N. Sakaya, V. Kmetik, Yo. Kato, M. Suzuki, M. Matsumura, J. Tajima, T. Nakayama, T. Wilhein. Opt. Commun., 163 (1-3), 103 (1999).
- [5] S. Kranzusch, K. Mann. Opt. Commun., 200 (1-6), 223 (2001).
- [6] A. Bartnik. Opto-Electronics Rev., 23 (2), 172 (2015).
- [7] F. Gilleron, M. Poirier, T. Blenski, M. Schmidt, T. Ceccotti. J. Appl. Phys., 94 (3), 2086 (2003).
- [8] H. Fiedorowicz, A. Bartnik, R. Jarocki, J. Kostecki, J. Krzywi.ski, J. Miko.ajczyk, R. Rakowski, A. Szczurek, M. Szczurek, J. Alloys Compounds, 401 (1-2), 99 (2005).
- [9] S. Kranzusch, K. Mann. Opt. Commun., 200 (1-6), 223 (2001).

- [10] A. Arikkatt, P.W. Wachulak, H. Fiedorowicz, A.S. Bartnik, J.L. Czwartos. Metrology and Measurement Systems, 27 (4), 701 (2020).
- [11] S.G. Kalmykov, P.S. Butorin, M.E. Sasin. J. Appl. Phys., **126** (10), 103301 (2019).
- [12] V.E. Levashov, K.N. Mednikov, A.S. Pirozhkov, E.N. Ragozin. Quant. Electron., 36 (6), 549 (2006).
- [13] M. Suzuki, H. Daido, I.W. Choi, W. Yu, K. Nagai, T. Nori-matsu, K. Mima, H. Fiedorowicz. Phys. Plasmas, 10 (1), 227 (2003).
- [14] P.S. Butorin, S.G. Kalmykov, V.A. Maximov, M.E. Sasin. J. Phys.: Conf. Ser., 1697 (1), 012237 (2020).
- [15] S.G. Kalmykov, P.S. Butorin, M.E. Sasin, V.S. Zakharov. J. Phys. D: Appl. Phys., 55 (10), 105203 (2022).
- [16] Yu.P. Raizer. UFN, 87 (9), 29 (1965) (in Russian).
- [17] D.A. Borisevichus, V.V. Zabrodskii, S.G. Kalmykov, M.E. Sasin, R.P. Seisyan. Pis'ma v ZhTF, 43 (1), 53 (2017) (in Russian). DOI: 10.21883/PJTF.2017.01.44089.16254
- [18] A.N. Nechay, A.A. Perekalov, N.I. Chkhalo, N.N. Salashchenko, I.G. Zabrodin, I.A. Kas'kov, A.E. Pestov. Poverkhnost'. Rentgenovskie, sinhrotronnye i neitronnye issledovaniya 9, 83 (2019) (in Russian).
- [19] M.A. Korepanov, M.R. Koroleva, E.A. Mitrukova. J. Phys.: Conf. Ser., 2057 (1), 012016 (2021).
- [20] A.V. Vodop'yanov, S.A. Garakhin, I.G. Zabrodin, S.Yu. Zuev, A.Ya. Lopatin, A.N. Nechay, N.I. Chkhalo. Kvant. elektron., 51 (8), (in Russian). 700 (2021).
- [21] V.E. Guseva, A.N. Nechay, A.A. Perekalov, N.N. Salashchenko, N.I. Chkhalo. Appl. Phys. B, 129 (10), 155 (2023).
- [22] A.N. Nechay, A.A. Perekalov, N.N. Salashchenko, N.I. Chkhalo. Opt. i spektr., 129 (3), 266 (2021) (in Russian).
- [23] A.N. Nechay, A.A. Perekalov, N.N. Salashchenko, N.I. Chkhalo. Opica i Spektroskopiya, 129 (2), 146 (2021) (in Russian).
- [24] P.S. Bytorin, S.G. Kalmykov, M.E. Sasin. Pisma v ZhTF, 44 (23), 111 (2018) (in Russian).
- [25] Yu.P. Raizer. Fizika Gazovogo Razryada (Nauka, M., 1987), p. 511.
- [26] B. Zeldovich, Yu. Raizer. Fizika udarnykh voln i vysokotemperaturnyh gidrodinamicheskih yavlenij (Ripol Klassik, 2013)

Translated by M.Shevelev